buildings

MDPI

Article

Soil–Structure Interaction Consideration for Base Isolated Structures under Earthquake Excitation

Arcan Yanik * and Yalcincan Ulus

Department of Civil Engineering, Istanbul Technical University, 34469 Istanbul, Turkey
* Correspondence: yanikar@itu.edu.tr; Tel.: +90-212-2856790

Abstract: This study aims to analytically implement base isolation with soil–structure interaction (SSI) on a sample structure and to develop a very simple solution to add these combined effects into the mass, damping and stiffness matrices of the structure. A spectrum analysis is also carried out considering the base-isolated structures and SSI. Dynamic simulations are performed throughout the study. In these simulations, three shear frame structures with different properties are considered. The strong ground motions selected for these analyses are eighteen different events with far-fault and near-fault components. In addition, four different base and soil structure combination cases are taken into account. These four analytical cases are a conventional structure with a fixed base and with SSI and a seismically isolated structure with or without the SSI. The numerical results showed that when SSI is considered, the effectiveness of the base isolation system may decrease, and the effect is prominent in softer soil conditions.

Keywords: base isolation; soil–structure interaction; earthquake; seismic; passive control

check for updates

Citation: Yanik, A.; Ulus, Y. Soil–Structure Interaction Consideration for Base Isolated Structures under Earthquake Excitation. *Buildings* **2023**, *13*, 915. https://doi.org/10.3390/buildings13040915

Academic Editor: Nerio Tullini

Received: 27 February 2023
Revised: 28 March 2023
Accepted: 29 March 2023
Published: 30 March 2023

1. Introduction

Base isolation (BI), also known as seismic isolation, is a widely used technique for protecting structures from earthquake effects. It is mostly used in critical facilities that need continuous operation even after severe earthquakes. Examples of these structures are hospitals, airports, nuclear power plants and government buildings. BI is also used in highway engineering structures such as bridges and viaducts. During earthquakes, the superstructure and the foundation are effectively decoupled from each other with the help of BI systems, resulting in much lower base shear forces and inter-story drifts [1].

Soil–structure interaction (SSI), also known as soil–foundation–structure interaction, is a design concept that takes the responses of structure, foundation and soil media into account. SSI is a concept that is often neglected in regard to design structures. Conventionally, structures are considered fixed to the ground, and the response of the underlying soil is neglected. This is because the effects of soil are usually considered beneficial to the structure, so neglecting soil can be considered conservative and safe. In FEMA 356 [2], soil–structure interaction is classified as a rare case that may modify the spectral response of the structure, particularly in soft soil conditions. There are two main approaches for evaluating SSI, one of which is the direct approach, where the soil is modeled as a continuum of the structure. The other is called the substructure approach, where the properties of soil are calculated via simple impedance functions or springs and dashpots. Soil properties that are calculated include the stiffness and damping characteristics of the soil–structure interaction. The substructure approach to impedance functions requires the foundation to be rigid and allows for the formulation of soil–structure interaction. In this paper, the substructure approach is used.

One of the first studies that investigated the effect of SSI in base-isolated structures was by Constantinou and Kneifati [3], who conducted a parametric study on a linear 1-degree-of-freedom structure. Bycroft [4] introduced approaching solutions and analysis

for the SSI when high frequencies are involved. Novak and Henderson [5] made use of the equations of motion for a structure by evaluating the SSI effect. Pappin et al. [6] highlighted the importance of the site effects on performance-based design. Mylonakis and Gazetas [7] investigated the use of SSI. They found that the effects of SSI are not necessarily beneficial and can be detrimental instead. Tongaonkar and Jangid [8] studied the effects of SSI on bridges. They concluded that considering SSI effects on isolated bridges is beneficial to the bridge and may result in cost reduction in design. When analyzing the damaging earthquake of 1999 in Athens, Mylonakis et al. [9] reached a conclusion that the effects of a surface layer made of soft rock and stiff soil were a detrimental factor. Syngros [10] analyzed the history of two different cases related to the seismic response of piles, supporting bridges and pile groups; the Ohba Ohashi bridge; and the Fukae Section of the Hanshin Expressway. He concluded that the type of soil changed the seismic waves, and the ground surface motion encountered by the specific bridge was greater; moreover, a higher frequency was measured in that portion. During the study of a 3D nonlinear model of BI, Deb [11] took SSI into consideration by using a near-fault earthquake. A detailed study related to an isolated structure and SSI with an unbounded section was conducted by Tsai et al. [12]. Dicleli et al. [13] studied the effects of SSI on two different types of bridges, one with heavy superstructure and light substructure and the other with opposite properties. They concluded that SSI effects should be investigated in soft soil conditions, regardless of the bridge type. Liu et al. [14] conducted a study in the time domain that investigates the effects of wind in high-rise structures with tuned mass dampers, considering SSI effects. They found that SSI affects the effectiveness of the dampers in soft soil conditions. Spyrakos et al. [15] studied the effects of SSI in buildings in the frequency domain. They found that SSI effects on the damping of the isolated structures are negligible, and the damping depends on BI damping characteristics.

Jeremic et al. [16] investigated the effects of SSI with varying soil properties on a four-span bridge. Karabörk et al. [17] conducted a study that investigates the effects of SSI on an isolated structure. Kausel [18] investigated the SSI history and phenomena. Genes et al. [19] conducted a study in order to analyze SSI effects in two different reinforced concrete buildings. Matinmanesh and Asheghabadi [20] took into consideration a plane finite element and used three different earthquake data with different frequency contents. They concluded that all types of soil have an effect on bedrock movement, but with different rates. Manolis and Markou [21] presented a combination of BI and SSI. They concluded that the BI performance depends on the type of soil. Giarlelis and Mylonakis [22] conducted a study related to the role of SSI in the elastic performance of multistory buildings. Li et al. [23] studied SSI in base-isolated structures in the frequency domain using the substructure approach. Luco [24] studied the effects of SSI on a structure that has a nonlinear BI system and concluded that SSI amplifies the response of the isolated structures. Tsai et al. [25] investigated the effects of SSI and damping in isolated structures. Yanik [26] proposed an instantaneous optimal control performance index for active control of structures under seismic excitation. Ashiquzzaman and Hong [27] studied the SSI effects on isolated nuclear power plant containment buildings. Zhou and Wei [28] conducted a similar study to Ashiquzzaman and Hong [27], where they studied SSI effects on nuclear power plants. They concluded that SSI directly affects the performance of isolation systems [28]. Xuefei et al. [29] investigated the optimal placement of passive control devices by considering SSI. Forcellini [30] studied the SSI effects on base-isolated buildings using OpenSees [31] framework and found that SSI effects are more pronounced in softer soil conditions. Dai et al. [32] studied the effects of SSI in a specific base-isolated bridge. They also found that in isolated structures, SSI effects are more pronounced. El-Sinawi [33] evaluated the effectiveness of magneto-rheological dampers and BI under seismic excitation. In a recent study, Yanik [34] mentioned that taking SSI into consideration reduces the effectiveness of magneto-rheological dampers. Zhenxia and Haiping [35] studied SSI effects on base-isolated structures using the finite element method. They found that the performance of BI systems is correlated with soil conditions. Some interesting recent numerical research about

SSI effects on tall buildings is presented by Forcellini [36]. As stated in [36], SSI effects have been extensively studied for low-rise buildings; however, SSI effects in tall buildings are a concept that needs to be investigated more. Another recent study on semi-active control by considering SSI is given by Jalali et al. [37]. Maleska and Beben [38] investigated the behavior of soil–steel composite bridges under earthquake excitation in their interesting research. Jishuai et al. [39] predicted the influence of SSI on reinforced concrete buildings by using neural networks. Liguo et al. [40] proposed a new framework for tuned mass damper systems with SSI effects. Yulin et al. [41] investigated the earthquake response of multi-span bridges by taking into account abutment–soil–foundation-structure interactions.

At present, there are a limited number of studies that investigate SSI and BI together, and the results of these studies are not always consistent with each other. This study aims to analyze SSI and BI effects on two-dimensional shear frame structures with the assumption of stories being rigid diaphragms. In addition, one of the most important aims of this paper is to analyze the SSI effect on high-rise buildings with base isolation. Furthermore, another aim is to analytically propose a new simple matrix formulation to study combined SSI effects and base isolation together and test the computational efficiency of this formulation. Analyses are conducted on three different shear frame structures, which are five, ten and forty stories high. The Newmark average acceleration method is used for dynamic analysis. In the next section, the formulation of the problem is presented.

2. Formulation of the Problem

In this section, the formulation of the problem is given in a detailed way. The Newmark average acceleration method is used for dynamic analysis. The soil model is defined below.

2.1. Representing Soil Structure

To take into account SSI in the analysis, the "spring and dashpot method" is used. Spring and dashpot analysis replaces the soil with springs and dashpots with horizontal, vertical, rotational and torsional degrees of freedom. In this study, the horizontal and rotational degrees of freedom are considered.

Calculations of the stiffness and damping coefficients of springs and dashpots are achieved by using the frequency-independent impedance functions [42]. As seen from the equations below, both structure and soil properties contribute to the calculations.

$$k_s = \frac{8Gr}{2-\nu} \tag{1}$$

$$k_r = \frac{8Gr^3}{3(1-\nu)} \tag{2}$$

$$c_s = \frac{4.6}{2-\nu}\rho V_S r^2 \tag{3}$$

$$c_r = \frac{0.4}{1-\nu}\rho V_S r^4 \tag{4}$$

In the equations above, the "s" subscript denotes "swaying", which is the horizontal component, and the "r" subscript denotes "rocking", which is the rotational component. k_s and k_r are swaying and rocking stiffness of the soil, respectively. Similarly, c_s and c_r are swaying and rocking and damping the soil, respectively. V_s, ρ and ν are the shear wave velocity, mass density and Poisson's ratio of the soil. G is the shear modulus of the soil, which can be calculated with the following equation:

$$G = \rho V_S^2 \tag{5}$$

r is the radius of the circular foundation. For a rectangular foundation with the dimensions of a and b, an equivalent r value can be calculated by equalizing areas of the rectangle and the circle, such that:

$$\pi r^2 = ab \tag{6}$$

$$r = \sqrt{\frac{ab}{\pi}} \tag{7}$$

The matrix formulation of the structure is defined below.

2.2. Matrix Formulation of the Structure

In this section, the formulation of the mass, stiffness and damping matrices of the structure is presented. In order to represent soil properties and BI in mass, stiffness and damping matrices, the corresponding values must be embedded into the matrices. An n-story fixed base shear building is shown in Figure 1. Conventional mass (**M**), damping (**C**) and stiffness (**K**) matrices for a fixed-based shear building can be written as:

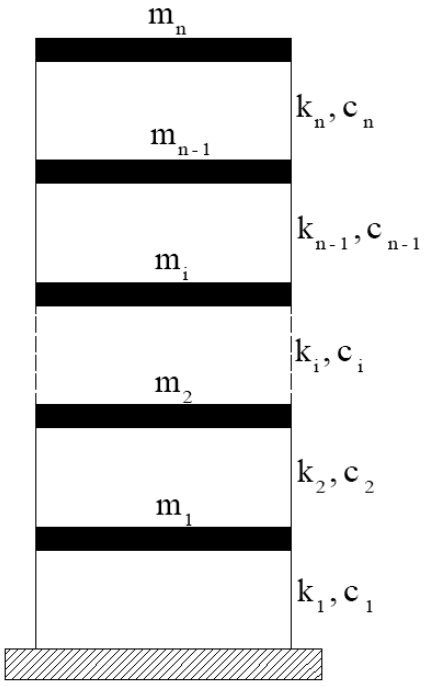

Figure 1. Fixed-based shear building.

$$\mathbf{M} = \begin{bmatrix} m_1 & 0 & 0 & \cdots & 0 \\ 0 & m_2 & 0 & \cdots & 0 \\ 0 & 0 & \ddots & \cdots & 0 \\ \vdots & \vdots & \vdots & m_{n-1} & 0 \\ 0 & 0 & 0 & 0 & m_n \end{bmatrix}_{n \times n} \tag{8}$$

$$\mathbf{C} = \begin{bmatrix} c_1 + c_2 & -c_2 & 0 & \cdots & 0 \\ -c_2 & c_2 + c_3 & -c_3 & \cdots & 0 \\ 0 & -c_3 & \ddots & \cdots & 0 \\ \vdots & \vdots & \vdots & c_{n-1} + c_n & -c_n \\ 0 & 0 & 0 & -c_n & c_n \end{bmatrix}_{n \times n} \tag{9}$$

$$\mathbf{K} = \begin{bmatrix} k_1 + k_2 & -k_2 & 0 & \cdots & 0 \\ -k_2 & k_2 + k_3 & -k_3 & \cdots & 0 \\ 0 & -k_3 & \ddots & \cdots & 0 \\ \vdots & \vdots & \vdots & k_{n-1} + k_n & -k_n \\ 0 & 0 & 0 & -k_n & k_n \end{bmatrix}_{n \times n} \tag{10}$$

where k_1 to k_n are the stiffnesses of the stories, c_1 to c_n are the damping of the stories, and m_1 to m_n are the mass of each story of an n-story structure. In the next section, the formulation for the base-isolated structure is presented.

2.3. Base Isolated Structure

The base-isolated shear building is shown in Figure 2. Properties of the BI can be implemented with the formulation given above by simply taking the BI layer as the first story of the structure.

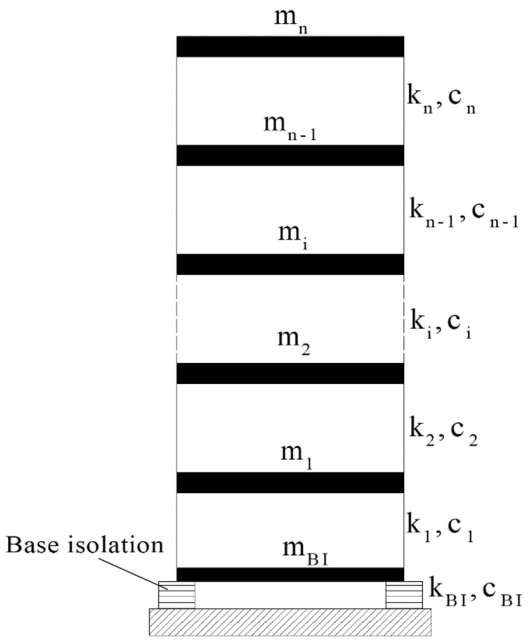

Figure 2. Base isolated shear building.

Mass ($\mathbf{M_{BI}}$), damping ($\mathbf{C_{BI}}$) and stiffness ($\mathbf{K_{BI}}$) matrices of a base-isolated n-story shear building can be written as:

$$\mathbf{M_{BI}} = \begin{bmatrix} m_{BI} & 0 & 0 & 0 & \cdots & 0 \\ 0 & m_1 & 0 & 0 & \cdots & 0 \\ 0 & 0 & m_2 & 0 & \cdots & 0 \\ 0 & 0 & 0 & \ddots & \cdots & 0 \\ \vdots & \vdots & \vdots & \vdots & m_{n-1} & 0 \\ 0 & 0 & 0 & 0 & 0 & m_n \end{bmatrix}_{(n+1) \times (n+1)} \tag{11}$$

$$\mathbf{C_{BI}} = \begin{bmatrix} c_{BI}+c_1 & -c_1 & 0 & 0 & \cdots & 0 \\ -c_1 & c_1+c_2 & -c_2 & 0 & \cdots & 0 \\ 0 & -c_2 & c_2+c_3 & -c_3 & \cdots & 0 \\ 0 & 0 & -c_3 & \ddots & \cdots & 0 \\ \vdots & \vdots & \vdots & \vdots & c_{n-1}+c_n & -c_n \\ 0 & 0 & 0 & 0 & -c_n & c_n \end{bmatrix}_{(n+1)\times(n+1)} \tag{12}$$

$$\mathbf{K_{BI}} = \begin{bmatrix} k_{BI}+k_1 & -k_1 & 0 & 0 & \cdots & 0 \\ -k_1 & k_1+k_2 & -k_2 & 0 & \cdots & 0 \\ 0 & -k_2 & k_2+k_3 & -k_3 & \cdots & 0 \\ 0 & 0 & -k_3 & \ddots & \cdots & 0 \\ \vdots & \vdots & \vdots & \vdots & k_{n-1}+k_n & -k_n \\ 0 & 0 & 0 & 0 & -k_n & k_n \end{bmatrix}_{(n+1)\times(n+1)} \tag{13}$$

where k_{BI} is the stiffness, c_{BI} is the damping and m_{BI} is the mass of the BI system. BI adds one degree of freedom to the fixed base structure; therefore, the dimensions of all matrices are increased by one. SSI implementation to the expressions given above is defined in the next section.

2.4. SSI Implementation

The spring–dashpot model of an n-story shear building considering SSI is shown in Figure 3. m_b and I_b are the mass and the mass moment of inertia of the foundation, respectively. I_1 to I_n are the mass moment of inertia of each floor. k_s is the swaying stiffness, k_r is the rocking stiffness, c_s is the swaying damping and c_r is the rocking damping of the foundation-soil medium. h_1 to h_n are story heights with respect to the ground. Swaying values are the horizontal components of the foundation–soil medium, whereas rocking values are rotational components. Mass, damping and stiffness matrices with SSI implementation can be written as follows [43]:

$$\mathbf{M_{SSI}} = \begin{bmatrix} \mathbf{M} & \mathbf{M_v} & \mathbf{M_h} \\ \mathbf{M_v^T} & \left(m_b + \sum_{i=1}^{n} m_i\right) & \left(\sum_{i=1}^{n} m_i h_i\right) \\ \mathbf{M_h^T} & \left(\sum_{i=1}^{n} m_i h_i\right) & \left(\sum_{i=1}^{n} m_i h_i^2 + I_b + \sum_{i=1}^{n} I_i\right) \end{bmatrix}_{(n+2)\times(n+2)} \tag{14}$$

$$\mathbf{C_{SSI}} = \begin{bmatrix} \mathbf{C} & 0 & 0 \\ 0 & c_s & 0 \\ 0 & 0 & c_r \end{bmatrix}_{(n+2)\times(n+2)} \tag{15}$$

$$\mathbf{K_{SSI}} = \begin{bmatrix} \mathbf{K} & 0 & 0 \\ 0 & k_s & 0 \\ 0 & 0 & k_r \end{bmatrix}_{(n+2)\times(n+2)} \tag{16}$$

where $\mathbf{M_{SSI}}$ is the mass matrix, $\mathbf{C_{SSI}}$ is the damping matrix and $\mathbf{K_{SSI}}$ is the stiffness matrix of the shear building considering SSI. In addition, $\mathbf{M_v}$ and $\mathbf{M_h}$ are defined as follows:

$$\mathbf{M_v} = \begin{bmatrix} m_1 \\ m_2 \\ \vdots \\ m_{n-1} \\ m_n \end{bmatrix}_{n\times 1} \tag{17}$$

$$\mathbf{M_h} = \begin{bmatrix} m_1 h_1 \\ m_2 h_2 \\ \vdots \\ m_{n-1} h_{n-1} \\ m_n h_n \end{bmatrix}_{n \times 1} \tag{18}$$

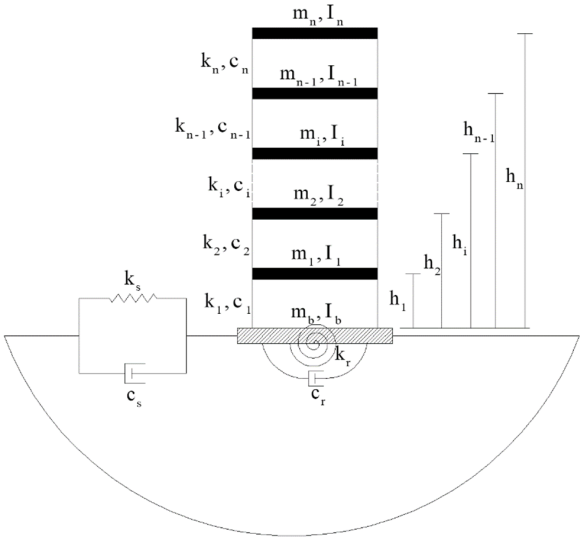

Figure 3. Shear building considering SSI.

SSI consideration implements two additional degrees of freedom to the fixed base structure; therefore, the dimensions of all matrices are increased by two. In the next section, the proposed simple formulation is presented.

2.5. Proposed Simple Formulation for SSI with Base Isolation

SSI in base-isolated structures can be represented by adjusting the SSI matrix formulation. This case is depicted in Figure 4. Fixed-based **M**, **C** and **K** matrices that are used in SSI matrices can be substituted with base-isolated $\mathbf{M_{BI}}$, $\mathbf{C_{BI}}$ and $\mathbf{K_{BI}}$ matrices. The height of the BI system, h_{BI}, must be included in the mass matrix considering SSI and BI together.

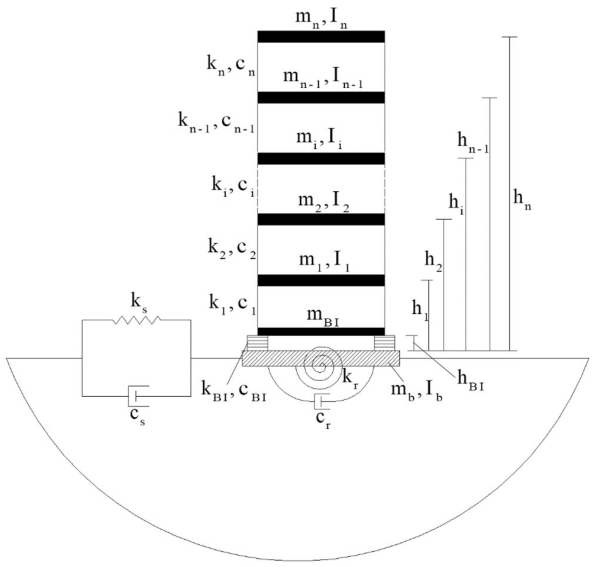

Figure 4. Shear building considering SSI and base isolation together.

The simple contribution of our research is the consideration of SSI and BI together in the formulation. With the help of an extensive number of numerical simulations that are performed by using many different earthquakes and soil types, it has been shown in the next sections that this type of formulation is computationally efficient. This simple formulation was not studied before. The details of the simple formulation are given below.

Mass, damping and stiffness matrices considering SSI and BI together can be written as follows:

$$\mathbf{M_{SSI,BI}} = \begin{bmatrix} \mathbf{M_{BI}} & \mathbf{M_{v,BI}} & \mathbf{M_{h,BI}} \\ \mathbf{M_{v,BI}^T} & \left(m_b + \sum_{i=1}^{n} m_i\right) & \left(\sum_{i=1}^{n} m_i h_i\right) \\ \mathbf{M_{h,BI}^T} & \left(\sum_{i=1}^{n} m_i h_i\right) & \left(\sum_{i=1}^{n} m_i h_i^2 + I_b + \sum_{i=1}^{n} I_i\right) \end{bmatrix}_{(n+3)\times(n+3)} \tag{19}$$

$$\mathbf{C_{SSI,BI}} = \begin{bmatrix} \mathbf{C_{BI}} & 0 & 0 \\ 0 & c_s & 0 \\ 0 & 0 & c_r \end{bmatrix}_{(n+3)\times(n+3)} \tag{20}$$

$$\mathbf{K_{SSI,BI}} = \begin{bmatrix} \mathbf{K_{BI}} & 0 & 0 \\ 0 & k_s & 0 \\ 0 & 0 & k_r \end{bmatrix}_{(n+3)\times(n+3)} \tag{21}$$

where $\mathbf{M_{SSI,BI}}$ is the mass matrix, $\mathbf{C_{SSI,BI}}$ is the damping matrix and $\mathbf{K_{SSI,BI}}$ is the stiffness matrix of the shear building considering SSI and BI together. $\mathbf{M_{v,BI}}$ and $\mathbf{M_{h,BI}}$ can be presented as:

$$\mathbf{M_{v,BI}} = \begin{bmatrix} m_{BI} \\ m_1 \\ m_2 \\ \vdots \\ m_{n-1} \\ m_n \end{bmatrix}_{(n+1)\times 1} \tag{22}$$

$$\mathbf{M_{h,BI}} = \begin{bmatrix} m_{BI}h_{BI} \\ m_1 h_1 \\ m_2 h_2 \\ \vdots \\ m_{n-1}h_{n-1} \\ m_n h_n \end{bmatrix}_{(n+1)\times 1} \tag{23}$$

While SSI introduces two additional degrees of freedom to the fixed base structure, BI adds one; therefore, the dimensions of all matrices are increased by three in total. Equations of the motion of the structure under seismic excitation are given below.

2.6. Equations of the Motion of the Structure under Earthquake Excitation

Four different equations of motion are presented in this section to cover all four analysis cases; these cases are fixed base, base-isolated, fixed base considering SSI and structure with BI considering SSI. The equation of motion for the fixed base analysis case can be written as follows:

$$\mathbf{M}(t) + \mathbf{C}\dot{u}(t) + \mathbf{K}u(t) = -\mathbf{m}^*{}_g(t) \tag{24}$$

where **m*** is a vector containing the diagonal of **M**, which happens to be the mass value

$$\mathbf{m}^* = \begin{bmatrix} m_1 \\ m_2 \\ \vdots \\ m_{n-1} \\ m_n \end{bmatrix}_{n\times 1} \tag{25}$$

Equations of motion for the base-isolated analysis case can be written by substituting the conventional fixed base matrices with a base-isolated matrix:

$$\mathbf{M_{BI}}(t) + \mathbf{C_{BI}}\dot{u}(t) + \mathbf{K_{BI}}u(t) = -\mathbf{m}^*_{\mathbf{BI}g}(t) \tag{26}$$

where $\mathbf{m}^*_{\mathbf{BI}}$ is a vector containing the diagonal elements of $\mathbf{M_{BI}}$:

$$\mathbf{m}^*_{\mathbf{BI}} = \begin{bmatrix} m_{BI} \\ m_1 \\ m_2 \\ \vdots \\ m_{n-1} \\ m_n \end{bmatrix}_{(n+1)\times 1} \tag{27}$$

$$\mathbf{M_{SSI}}(t) + \mathbf{C_{SSI}}\dot{u}(t) + \mathbf{K_{SSI}}u(t) = -\mathbf{m}^*_{\mathbf{SSI}g}(t) \tag{28}$$

where $\mathbf{m}^*_{\mathbf{SSI}}$ is a vector containing the diagonal elements of $\mathbf{M}$ with $(m_b + \sum_{i=1}^{n} m_i)$ and $(\sum_{i=1}^{n} m_i h_i)$ from $\mathbf{M_{SSI}}$ [43]:

$$\mathbf{m}^*_{\mathbf{SSI}} = \begin{bmatrix} m_1 \\ m_2 \\ \vdots \\ m_{n-1} \\ m_n \\ \left(m_b + \sum\limits_{i=1}^{n} m_i\right) \\ \left(\sum\limits_{i=1}^{n} m_i h_i\right) \end{bmatrix}_{(n+2)\times 1} \tag{29}$$

For the joint case of SSI and BI, the equation of motion is presented as given below:

$$\mathbf{M_{SSI,BI}}(t) + \mathbf{C_{SSI,BI}}\dot{u}(t) + \mathbf{K_{SSI,BI}}u(t) = -\mathbf{m}^*_{\mathbf{SSI,BI}g}(t) \tag{30}$$

where $\mathbf{m}^*_{\mathbf{SSI,BI}}$ is a vector containing the diagonal of $\mathbf{M_{BI}}$ with the additions of $(m_b + \sum_{i=1}^{n} m_i)$ and $(\sum_{i=1}^{n} m_i h_i)$ from $\mathbf{M_{SSI,BI}}$ [43]:

$$\mathbf{m}^*_{\mathbf{SSI,BI}} = \begin{bmatrix} m_{BI} \\ m_1 \\ m_2 \\ \vdots \\ m_{n-1} \\ m_n \\ \left(m_b + \sum\limits_{i=1}^{n} m_i\right) \\ \left(\sum\limits_{i=1}^{n} m_i h_i\right) \end{bmatrix}_{(n+3)\times 1} \tag{31}$$

In the equations defined above, $_g(t)$ is the horizontal ground motion acceleration. $u(t)$, (t) and (t) are the displacement, velocity and acceleration vectors of the structure.

In order to perform the dynamic analysis under seismic excitation with or without consideration of SSI and by taking into account all base conditions, the following approach was used. The mathematical equations defined in this section are implemented in a code that was created in MATLAB software. The accuracy of the MATLAB code was checked by comparing the results with SAP2000 software by considering a simple shear building example. Moreover, MATLAB code did not create any instability problems during the performance of an extensive number of simulations. It was fast and efficient by using the proposed simple formula defined in Section 2.5. A numerical example is defined in the next section.

3. Numerical Example

Analyses were carried out on three different shear frame structures, which have five, ten and forty stories. For each building, four different base conditions were considered. These conditions consist of a fixed base, an isolated base, an SSI-included base and an isolated base considering SSI. The models of these cases are shown in Figures 1–4, respectively. It should be noted here that Figures 1–4 represent general cases and are created for buildings with n number of stories. For SSI cases, four different soil conditions, very soft, soft, medium and dense, are considered. All cases are tested with a suite of earthquakes with different rupture distances. Soil properties of each building can be calculated with the equations listed in Section 2.1. Soil properties are taken and adapted from [14], which have been used in different studies previously [43–45]. Soil properties of five-and ten-story buildings are the same because the foundation dimensions are the same. Soil properties are given in Table 1. Soil properties of five- and ten-story buildings are given in Table 2. Soil properties of the forty-story building are given in Table 3. Three different shear frame buildings are used in the analysis. Building properties of the forty-story building, five-story building and ten-story building are given in Tables 4–6, respectively. Building properties are chosen by us to be in line with real-life building properties. Base isolation properties such as mass m_b, stiffness k_b and damping c_b are calculated with the following expressions. In the equations below, m is the mass, and k is the stiffness of the first story above the isolation level. m, k and c values are given in Tables 4–6. The following equation is taken from [1]. The critical damping ratio for base isolation is taken as 10%.

$$\begin{array}{c} m_b = m;\ k_b = 0.05k; \\ c_b = \xi_b 2\sqrt{m_{total}\ k_b} \end{array} \quad (32)$$

Table 1. Soil properties.

Soil	ν	ρ ton/m^3	V_S m/s^2	G kN/m^2
Very Soft	0.49	1.60	50	4000
Soft	0.49	1.80	100	18,000
Medium	0.48	1.90	300	171,000
Dense	0.33	2.40	500	600,000

Table 2. Soil properties of the five- and ten-story buildings.

Soil	k_s kN/m	k_r kN/m	c_s kNs/m	c_r kNs/m
Very Soft	2.39×10^5	3.00×10^7	3.49×10^5	1.01×10^6
Soft	1.07×10^6	1.35×10^8	7.87×10^5	2.28×10^6
Medium	1.02×10^7	1.26×10^9	2.47×10^6	7.09×10^6
Dense	3.24×10^7	3.43×10^9	4.74×10^6	1.16×10^7

Table 3. Soil properties of the forty-story buildings.

Soil	k_s kN/m	k_r kN/m	c_s kNs/m	c_r kNs/m
Very Soft	4.78×10^5	2.40×10^8	2.79×10^6	1.62×10^7
Soft	2.15×10^6	1.08×10^9	6.30×10^6	3.66×10^7
Medium	2.03×10^7	1.01×10^{10}	1.98×10^7	1.14×10^8
Dense	6.48×10^7	2.74×10^{10}	3.79×10^7	1.86×10^8

Table 4. Properties of the forty-story building.

story height, h_i (m)	4 to 160
story mass, m_i (ton)	980
story stiffness, k_i (kN/m)	2.1×10^6 to 0.99×10^6
story damping, c_i (kNs/m)	42.6×10^3 to 20×10^3
story inertia, I_i (ton·m^2)	1.31×10^5
foundation mass, m_0 (ton)	1960
foundation inertia, I_0 (ton·m^2)	1.96×10^5

Table 5. Properties of the five-story building.

story height, h_i (m)	4 to 20
story mass, m_i (ton)	300
story stiffness, k_i (kN/m)	3.5×10^5 to 1.50×10^5
story inertia, I_i (ton·m^2)	7.5×10^3
foundation mass, m_0 (ton)	300
foundation inertia, I_0 (ton·m^2)	7.5×10^5

Table 6. Properties of the ten-story building.

story height, h_i (m)	4 to 40
story mass, m_i (ton)	300
story stiffness, k_i (kN/m)	7.0×10^5 to 3.00×10^5
story inertia, I_i (ton·m^2)	7.5×10^3
foundation mass, m_0 (ton)	300
foundation inertia, I_0 (ton·m^2)	7.5×10^5

A large number of earthquakes are used in the analysis. All the earthquake data were downloaded from the PEER Ground Motion Database [46]. Corresponding earthquakes include near-field records with rupture distances of less than 20 km and far-field records with rupture distances of more than 20 km. Earthquake events used in this study are listed in Table 7. The specific earthquake recording names and recording station information are presented in the first two columns of Table 8. The number of records can also be obtained from Table 8. Table 8 is given in the next section. More information about consistent approaches in selecting earthquake records for seismic hazard mitigation studies can be obtained from [47–49]. Moreover, the most recent approaches concerning base isolation systems can be found in [50].

We wanted to compare different soil cases with uniform building and uniform base isolation parameters. Therefore, we used the same type of base isolation properties in every building and soil type in this study.

Dynamic simulations are performed by using Newmark's average acceleration time stepping method. In addition to time history analysis, spectrum analysis was also conducted. In the following section, numerical results that were obtained by performing dynamic simulations using the sample building defined in this section are presented. The earthquakes defined in Table 7 are also used in the following section.

Table 7. Earthquake events considered in the analysis.

Event	Year	Magnitude (M_w)	Mechanism
Imperial Valley, US	1940	6.95	Strike Slip
Imperial Valley, US	1979	6.53	Strike Slip
Loma Prieta, US	1989	6.93	Reverse Oblique
Manjil, IR	1990	7.37	Strike Slip
Cape Mendocino, US	1992	7.01	Reverse
Erzincan, TR	1992	6.69	Strike Slip
Northridge, US	1994	6.69	Reverse
Dinar, TR	1995	6.40	Normal
Kobe, JP	1995	6.90	Strike Slip
Chi-Chi, TW	1999	7.62	Reverse Oblique
Düzce, TR	1999	7.14	Strike Slip
Hector Mine, US	1999	7.13	Strike Slip
Kocaeli, TR	1999	7.51	Strike Slip
Iwate, JP	2008	6.90	Reverse
Darfield, NZ	2010	7.00	Strike Slip
El Mayor Cucapah, MX	2010	7.20	Strike Slip
Christchurch, NZ	2011	6.20	Reverse Oblique

Table 8. Maximum roof displacement values of the ten-story building.

Earthquake	Station	Soil	Fixed (m)	BI (m)	BI Reduction (%)	SSI (m)	SSI_BI (m)	BI Reduction w/SSI (%)
Imperial Valley, 1940	El Centro Array #9	Very Soft	0.185	0.078	57.86	0.075	0.053	29.29
Imperial Valley, 1940	El Centro Array #9	Soft	0.185	0.078	57.86	0.101	0.078	23.07
Imperial Valley, 1940	El Centro Array #9	Medium	0.185	0.078	57.86	0.163	0.078	52.06
Imperial Valley, 1940	El Centro Array #9	Dense	0.185	0.078	57.86	0.179	0.078	56.26
Imperial Valley, 1979	Calipatria Fire Station	Very Soft	0.070	0.022	68.48	0.022	0.016	26.70
Imperial Valley, 1979	Calipatria Fire Station	Soft	0.070	0.022	68.48	0.028	0.019	32.25
Imperial Valley, 1979	Calipatria Fire Station	Medium	0.070	0.022	68.48	0.057	0.022	61.18
Imperial Valley, 1979	Calipatria Fire Station	Dense	0.070	0.022	68.48	0.069	0.022	68.11
Imperial Valley, 1979	Delta	Very Soft	0.103	0.051	50.32	0.053	0.046	12.30
Imperial Valley, 1979	Delta	Soft	0.103	0.051	50.32	0.063	0.044	29.62
Imperial Valley, 1979	Delta	Medium	0.103	0.051	50.32	0.084	0.051	39.14
Imperial Valley, 1979	Delta	Dense	0.103	0.051	50.32	0.093	0.051	44.87
Loma Prieta, 1989	Alameda Naval Air Stn Hanger	Very Soft	0.195	0.036	81.59	0.026	0.030	−14.31
Loma Prieta, 1989	Alameda Naval Air Stn Hanger	Soft	0.195	0.036	81.59	0.067	0.038	43.62
Loma Prieta, 1989	Alameda Naval Air Stn Hanger	Medium	0.195	0.036	81.59	0.162	0.036	77.66
Loma Prieta, 1989	Alameda Naval Air Stn Hanger	Dense	0.195	0.036	81.59	0.185	0.036	80.52
Loma Prieta, 1989	Capitola	Very Soft	0.261	0.057	78.07	0.102	0.043	57.31
Loma Prieta, 1989	Capitola	Soft	0.261	0.057	78.07	0.235	0.060	74.32
Loma Prieta, 1989	Capitola	Medium	0.261	0.057	78.07	0.238	0.059	75.32
Loma Prieta, 1989	Capitola	Dense	0.261	0.057	78.07	0.256	0.058	77.38
Erzincan, 1992 (EW)	Erzincan	Very Soft	0.516	0.250	51.55	0.232	0.197	15.14
Erzincan, 1992 (EW)	Erzincan	Soft	0.516	0.250	51.55	0.374	0.244	34.67
Erzincan, 1992 (EW)	Erzincan	Medium	0.516	0.250	51.55	0.481	0.250	47.90
Erzincan, 1992 (EW)	Erzincan	Dense	0.516	0.250	51.55	0.494	0.250	49.31
Erzincan, 1992 (NS)	Erzincan	Very Soft	0.571	0.249	56.40	0.231	0.196	15.26
Erzincan, 1992 (NS)	Erzincan	Soft	0.571	0.249	56.40	0.372	0.243	34.74
Erzincan, 1992 (NS)	Erzincan	Medium	0.571	0.249	56.40	0.479	0.249	47.95
Erzincan, 1992 (NS)	Erzincan	Dense	0.571	0.249	56.40	0.533	0.249	53.29
Cape Mendocino, 1992	Cape Mendocino	Very Soft	0.285	0.106	62.85	0.126	0.111	12.50
Cape Mendocino, 1992	Cape Mendocino	Soft	0.285	0.106	62.85	0.194	0.108	44.37
Cape Mendocino, 1992	Cape Mendocino	Medium	0.285	0.106	62.85	0.256	0.106	58.53
Cape Mendocino, 1992	Cape Mendocino	Dense	0.285	0.106	62.85	0.276	0.106	61.57
Cape Mendocino, 1992	Shelter Cove Airport	Very Soft	0.009	0.004	52.19	0.006	0.003	50.17

Table 8. *Cont.*

Earthquake	Station	Soil	Fixed (m)	BI (m)	BI Reduction (%)	SSI (m)	SSI_BI (m)	BI Reduction w/SSI (%)
Cape Mendocino, 1992	Shelter Cove Airport	Soft	0.009	0.004	52.19	0.006	0.003	41.20
Cape Mendocino, 1992	Shelter Cove Airport	Medium	0.009	0.004	52.19	0.008	0.004	44.65
Cape Mendocino, 1992	Shelter Cove Airport	Dense	0.009	0.004	52.19	0.009	0.004	50.99
Northridge, 1994	Anacapa Island	Very Soft	0.017	0.002	85.23	0.005	0.002	59.54
Northridge, 1994	Anacapa Island	Soft	0.017	0.002	85.23	0.007	0.002	71.38
Northridge, 1994	Anacapa Island	Medium	0.017	0.002	85.23	0.014	0.002	83.04
Northridge, 1994	Anacapa Island	Dense	0.017	0.002	85.23	0.016	0.002	84.52
Northridge, 1994	Canoga Park	Very Soft	0.637	0.320	49.77	0.297	0.252	15.26
Northridge, 1994	Canoga Park	Soft	0.637	0.320	49.77	0.478	0.312	34.73
Northridge, 1994	Canoga Park	Medium	0.637	0.320	49.77	0.614	0.320	47.87
Northridge, 1994	Canoga Park	Dense	0.637	0.320	49.77	0.631	0.320	49.24
Kobe, 1995	Abeno	Very Soft	0.107	0.025	76.62	0.034	0.016	53.33
Kobe, 1995	Abeno	Soft	0.107	0.025	76.62	0.058	0.024	58.10
Kobe, 1995	Abeno	Medium	0.107	0.025	76.62	0.080	0.025	68.67
Kobe, 1995	Abeno	Dense	0.107	0.025	76.62	0.097	0.025	74.17
Kobe, 1995	HIK	Very Soft	0.103	0.029	71.54	0.032	0.016	48.03
Kobe, 1995	HIK	Soft	0.103	0.029	71.54	0.076	0.022	71.56
Kobe, 1995	HIK	Medium	0.103	0.029	71.54	0.092	0.029	68.64
Kobe, 1995	HIK	Dense	0.103	0.029	71.54	0.099	0.029	70.56
Dinar, 1995	Balikesir	Very Soft	0.005	0.002	60.24	0.003	0.001	52.65
Dinar, 1995	Balikesir	Soft	0.005	0.002	60.24	0.007	0.002	74.38
Dinar, 1995	Balikesir	Medium	0.005	0.002	60.24	0.005	0.002	65.64
Dinar, 1995	Balikesir	Dense	0.005	0.002	60.24	0.005	0.002	62.85
Dinar, 1995	Dinar	Very Soft	0.309	0.110	64.31	0.156	0.061	61.02
Dinar, 1995	Dinar	Soft	0.309	0.110	64.31	0.225	0.103	54.45
Dinar, 1995	Dinar	Medium	0.309	0.110	64.31	0.269	0.110	59.31
Dinar, 1995	Dinar	Dense	0.309	0.110	64.31	0.306	0.110	64.02
Kocaeli, 1999	Arcelik	Very Soft	0.053	0.016	70.20	0.017	0.014	16.73
Kocaeli, 1999	Arcelik	Soft	0.053	0.016	70.20	0.034	0.016	53.71
Kocaeli, 1999	Arcelik	Medium	0.053	0.016	70.20	0.052	0.016	69.52
Kocaeli, 1999	Arcelik	Dense	0.053	0.016	70.20	0.053	0.016	70.43
Kocaeli, 1999	Istanbul	Very Soft	0.014	0.010	31.95	0.009	0.009	1.23
Kocaeli, 1999	Istanbul	Soft	0.014	0.010	31.95	0.016	0.010	40.94
Kocaeli, 1999	Istanbul	Medium	0.014	0.010	31.95	0.014	0.010	28.99
Kocaeli, 1999	Istanbul	Dense	0.014	0.010	31.95	0.013	0.010	25.07
Chi-Chi, 1999	CHY006	Very Soft	0.362	0.073	79.85	0.087	0.060	31.67
Chi-Chi, 1999	CHY006	Soft	0.362	0.073	79.85	0.183	0.071	61.13
Chi-Chi, 1999	CHY006	Medium	0.362	0.073	79.85	0.344	0.073	78.76
Chi-Chi, 1999	CHY006	Dense	0.362	0.073	79.85	0.357	0.073	79.57
Chi-Chi, 1999	CHY101	Very Soft	0.216	0.080	62.68	0.092	0.103	−11.95
Chi-Chi, 1999	CHY101	Soft	0.216	0.080	62.68	0.103	0.094	8.96
Chi-Chi, 1999	CHY101	Medium	0.216	0.080	62.68	0.173	0.082	52.78
Chi-Chi, 1999	CHY101	Dense	0.216	0.080	62.68	0.197	0.081	58.97
Duzce, 1999	Bursa	Very Soft	0.848	0.433	48.95	0.401	0.341	15.03
Duzce, 1999	Bursa	Soft	0.848	0.433	48.95	0.643	0.422	34.35
Duzce, 1999	Bursa	Medium	0.848	0.433	48.95	0.820	0.433	47.22
Duzce, 1999	Bursa	Dense	0.848	0.433	48.95	0.840	0.433	48.45
Duzce, 1999	Duzce	Very Soft	0.632	0.316	49.95	0.295	0.249	15.42
Duzce, 1999	Duzce	Soft	0.632	0.316	49.95	0.474	0.309	34.88
Duzce, 1999	Duzce	Medium	0.632	0.316	49.95	0.610	0.317	48.03
Duzce, 1999	Duzce	Dense	0.632	0.316	49.95	0.626	0.317	49.42
Manjil, 1990	Abbar	Very Soft	0.110	0.079	28.09	0.061	0.060	1.50
Manjil, 1990	Abbar	Soft	0.110	0.079	28.09	0.078	0.087	−10.94
Manjil, 1990	Abbar	Medium	0.110	0.079	28.09	0.092	0.082	10.35
Manjil, 1990	Abbar	Dense	0.110	0.079	28.09	0.099	0.081	18.94
Manjil, 1990	Rudsar	Very Soft	0.057	0.015	73.12	0.026	0.012	55.12
Manjil, 1990	Rudsar	Soft	0.057	0.015	73.12	0.053	0.015	71.25
Manjil, 1990	Rudsar	Medium	0.057	0.015	73.12	0.061	0.015	75.50
Manjil, 1990	Rudsar	Dense	0.057	0.015	73.12	0.058	0.015	73.63
Hector Mine, 1999	Banning	Very Soft	0.011	0.006	40.51	0.006	0.004	34.64
Hector Mine, 1999	Banning	Soft	0.011	0.006	40.51	0.006	0.006	8.82
Hector Mine, 1999	Banning	Medium	0.011	0.006	40.51	0.010	0.006	35.18
Hector Mine, 1999	Banning	Dense	0.011	0.006	40.51	0.010	0.006	38.88
Hector Mine, 1999	Indio	Very Soft	0.073	0.044	39.99	0.046	0.035	24.68

Table 8. *Cont.*

Earthquake	Station	Soil	Fixed (m)	BI (m)	BI Reduction (%)	SSI (m)	SSI_BI (m)	BI Reduction w/SSI (%)
Hector Mine, 1999	Indio	Soft	0.073	0.044	39.99	0.082	0.046	43.52
Hector Mine, 1999	Indio	Medium	0.073	0.044	39.99	0.067	0.044	34.91
Hector Mine, 1999	Indio	Dense	0.073	0.044	39.99	0.071	0.044	38.34
Iwate, 2008	AKT023	Very Soft	0.186	0.036	80.50	0.043	0.030	31.37
Iwate, 2008	AKT023	Soft	0.186	0.036	80.50	0.085	0.035	58.73
Iwate, 2008	AKT023	Medium	0.186	0.036	80.50	0.161	0.036	77.71
Iwate, 2008	AKT023	Dense	0.186	0.036	80.50	0.179	0.036	79.83
Iwate, 2008	IWT010	Very Soft	0.139	0.067	51.61	0.062	0.043	30.69
Iwate, 2008	IWT010	Soft	0.139	0.067	51.61	0.080	0.065	18.65
Iwate, 2008	IWT010	Medium	0.139	0.067	51.61	0.129	0.068	46.80
Iwate, 2008	IWT010	Dense	0.139	0.067	51.61	0.137	0.068	50.50
El Mayor-Cucapah, 2010	Chihuahua	Very Soft	0.133	0.040	69.61	0.038	0.053	−38.85
El Mayor-Cucapah, 2010	Chihuahua	Soft	0.133	0.040	69.61	0.134	0.046	65.74
El Mayor-Cucapah, 2010	Chihuahua	Medium	0.133	0.040	69.61	0.138	0.041	70.22
El Mayor-Cucapah, 2010	Chihuahua	Dense	0.133	0.040	69.61	0.142	0.041	71.50
El Mayor-Cucapah, 2010	Michoacan de Ocampo	Very Soft	0.332	0.113	65.99	0.107	0.095	11.68
El Mayor-Cucapah, 2010	Michoacan de Ocampo	Soft	0.332	0.113	65.99	0.184	0.117	36.35
El Mayor-Cucapah, 2010	Michoacan de Ocampo	Medium	0.332	0.113	65.99	0.276	0.114	58.63
El Mayor-Cucapah, 2010	Michoacan de Ocampo	Dense	0.332	0.113	65.99	0.315	0.113	63.95
Darfield, 2010	Canterbury Aero Club	Very Soft	0.056	0.037	35.09	0.045	0.029	34.56
Darfield, 2010	Canterbury Aero Club	Soft	0.056	0.037	35.09	0.052	0.039	24.88
Darfield, 2010	Canterbury Aero Club	Medium	0.056	0.037	35.09	0.050	0.037	25.14
Darfield, 2010	Canterbury Aero Club	Dense	0.056	0.037	35.09	0.053	0.037	30.06
Darfield, 2010	DSLC	Very Soft	0.218	0.064	70.61	0.053	0.046	12.41
Darfield, 2010	DSLC	Soft	0.218	0.064	70.61	0.071	0.071	0.30
Darfield, 2010	DSLC	Medium	0.218	0.064	70.61	0.196	0.066	66.20
Darfield, 2010	DSLC	Dense	0.218	0.064	70.61	0.215	0.065	69.82
Christchurch, 2011	ADCS	Very Soft	0.017	0.003	81.89	0.006	0.003	46.34
Christchurch, 2011	ADCS	Soft	0.017	0.003	81.89	0.006	0.003	49.92
Christchurch, 2011	ADCS	Medium	0.017	0.003	81.89	0.014	0.003	78.63
Christchurch, 2011	ADCS	Dense	0.017	0.003	81.89	0.016	0.003	80.98
Christchurch, 2011	CECS	Very Soft	0.009	0.006	38.67	0.009	0.003	64.57
Christchurch, 2011	CECS	Soft	0.009	0.006	38.67	0.007	0.004	31.37
Christchurch, 2011	CECS	Medium	0.009	0.006	38.67	0.008	0.006	30.16
Christchurch, 2011	CECS	Dense	0.009	0.006	38.67	0.009	0.006	36.30

4. Numerical Results

The numerical results section is concentrated on the acceleration, velocity and displacement time histories of the structures. Dynamic simulations are performed for every soil condition given above. In addition, the results are presented separately for each soil condition. The comparisons are carried out between the conventional structures and the structure with BI. Figure 5 shows the top story acceleration time history responses of the five-story building for the 1989 Loma Prieta Earthquake, considering different soil conditions. We should mention here that the accelerations are relative accelerations and not absolute acceleration responses. The maximum velocities are also investigated, but they are not shown here, and no comparative velocity analysis is given in this section because of space constraints. However, for all mentioned earthquakes, building heights and soil cases mentioned in this paper earlier, the velocity investigation is carried out, and the outcomes are considered in the conclusion section. The displacement time histories for different soil conditions for the five-story building under the effect of the Loma Prieta earthquake and the maximum displacement of each story are not shown for this building, as the maximum roof displacements for every case defined are shown in Table 8. The maximum displacement

curves are only shown for the forty-story building in this section. Figure 6 shows the maximum relative acceleration of the ten-story building under the effect of the Kocaeli 1999 earthquake. The top story displacement time history for the ten-story building under the effect of the Kocaeli earthquake is given in Figure 7. For the forty-story building under the effect of the 1979 Imperial Valley Earthquake, the top story acceleration time histories and maximum acceleration of each story are shown in Figures 8 and 9, respectively. Moreover, in Figure 10, the top story displacement time histories are shown, while in Figure 11, the maximum story displacements are presented for the 1979 Imperial Valley earthquake.

Considering the acceleration results (the majority of the results are not shown in this paper) for five-, ten- and forty-story buildings, BI reduces the responses significantly in all cases. This is more of an expected outcome. In addition, SSI reduces the acceleration values, but these effects are only pronounced in softer soil conditions. Considering the velocity curves for five-, ten- and forty-story buildings (these curves are not shown here), the results are similar to the acceleration results; BI reduces the responses considerably. It can also be claimed that SSI reduces the velocity values, but again, these effects are only pronounced in softer soil conditions. In very soft soil conditions, SSI effects can be observed clearly, but when moving towards denser soil, the effects disappear, and the structures behave like they are fixed based.

Considering the displacement results for five-, ten- and forty-story buildings, although the base isolated displacements might be higher than in fixed base cases, large displacements occur at the BI layer, providing low inter-story displacements, and the structures behave linearly. This may also mean that the BI absorbs most of the seismic energy by itself. However, an energy-based analysis was not carried out here. This is also an anticipated characteristic of BI. It can also be mentioned that SSI reduces the displacement values; like the acceleration and velocity investigations, these effects are only pronounced in softer soil conditions. This is the expected result, as the dense soil case has the closest behavior to a fixed base case among all soil cases studied in this paper.

Maximum roof displacement values were calculated for each earthquake, and results for the ten-story building are presented in Table 8. More specific outcomes with numerical percentages are given in this part. For the base isolated case, the displacement of the isolation system was subtracted from the story displacements. The sixth column of Table 8 shows the fixed base response reduction percentage of the base isolated case. For this comparison, SSI was not included. Without considering SSI in the base isolated cases, the response reduction percentage ranges from 28% to 85%, which is a significant maximum reduction percentage. If we consider the ninth column of Table 8, which is the base response reduction percentage of the base isolated case considering SSI, this case compares the structure without BI with SSI and the structure with BI considering SSI. For this case, the response reduction ranges from −38% to almost 85%. Moreover, −38% corresponds to the El Mayor-Cucapah 2010 earthquake and is a very soft soil condition case. Additionally, this percentage shows that BI increased the uncontrolled structure displacement. However, this is one of the only four extreme cases out of 132 analyses. We only wanted to interpret the negative percentage meaning here. However, if the ninth column is considered specifically, it tells us that BI usage still significantly decreases the responses of upper stories, although these reductions are not as high as in the cases in which SSI is not considered. Another important finding from this table, which can be seen clearly, is that for dense soil cases, the response reductions are almost identical to those for the fixed base cases. If we compare the sixth and ninth columns of Table 8, the difference in the response reduction percentage for the fixed base case and dense soil case ranges from 9% to −2%. Furthermore, −2% means that in one of the dense soil cases, the response reduction is higher than in the case without SSI. This may also be considered as one of the four extreme cases and not an expected result.

It can be understood from the results that the effectiveness of BI is generally reduced when SSI is considered. Only 12 out of 132 analyses showed that the BI reduction is clearly increased considering SSI. In the next section, the BI spectrum is given.

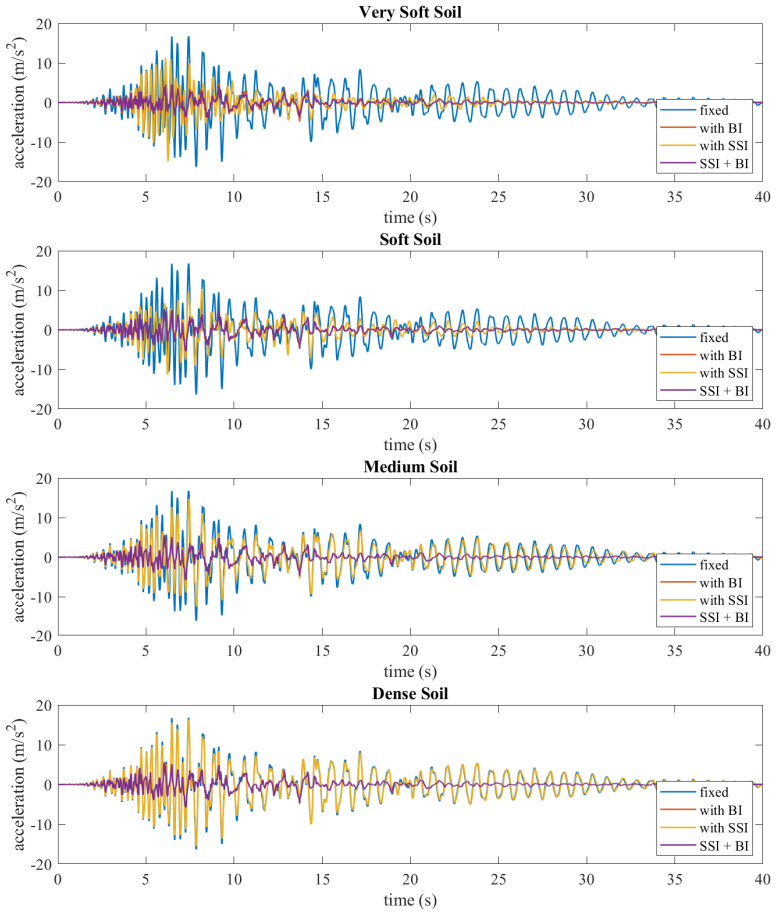

Figure 5. Top story acceleration–time history of five-story buildings (Loma Prieta, 1989).

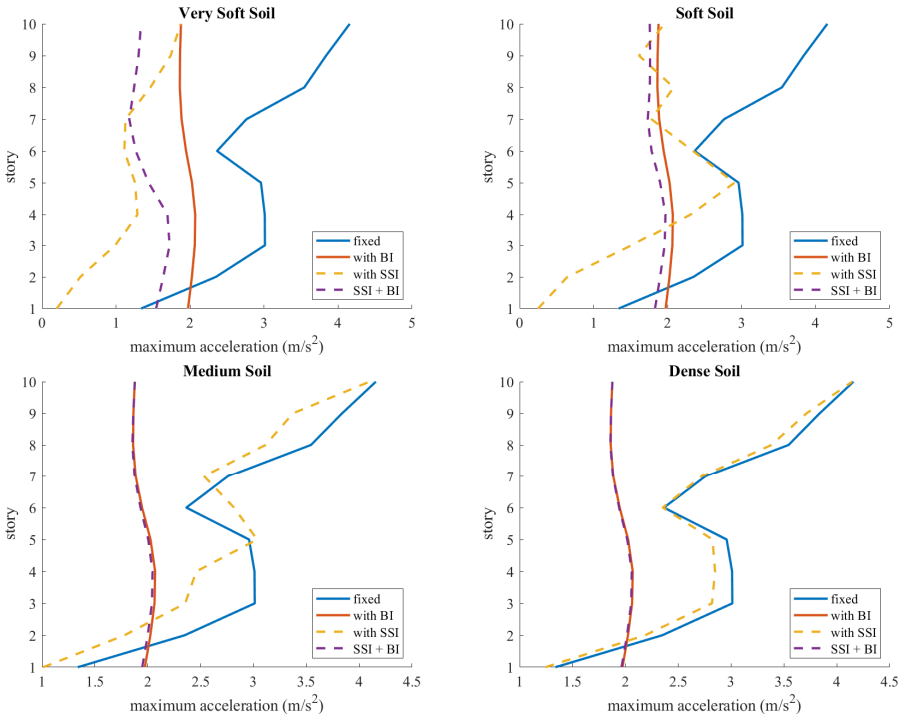

Figure 6. Maximum acceleration of each story for the ten-story building (Kocaeli, 1999).

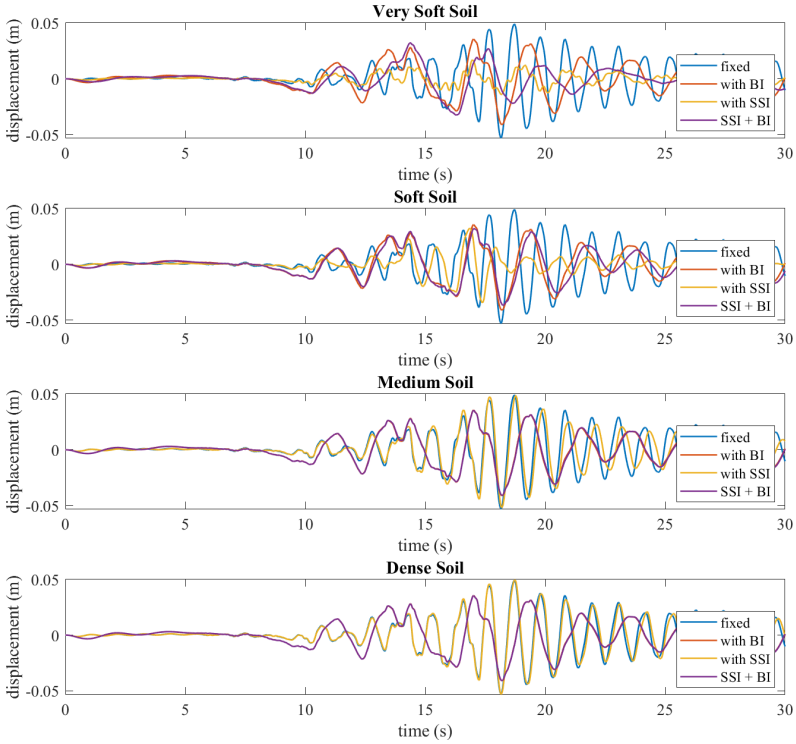

Figure 7. Top story displacement–time history of the ten-story building (Kocaeli, 1999).

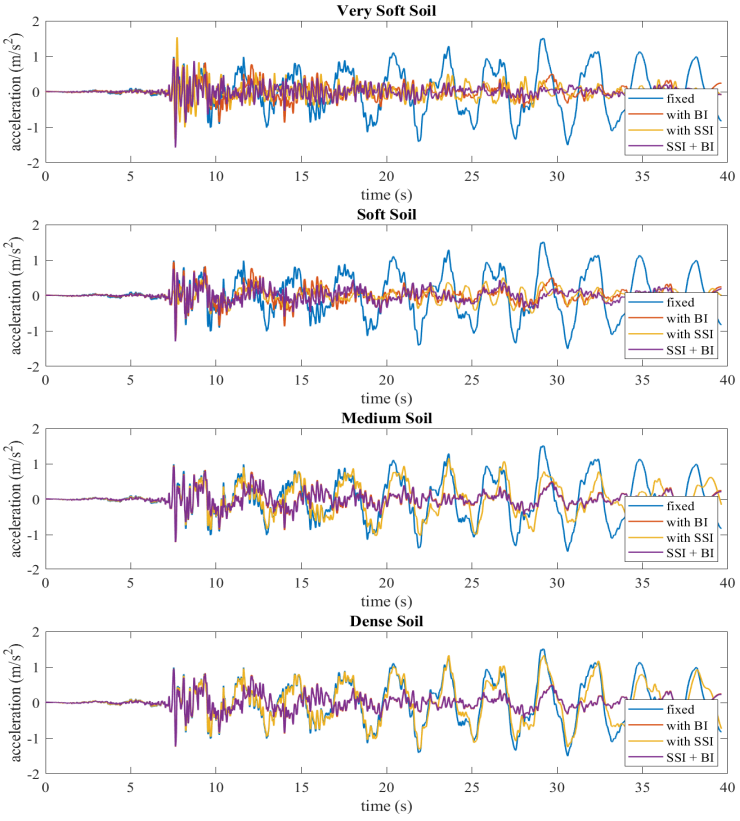

Figure 8. Top story acceleration–time history of forty-story buildings (Imperial Valley, 1979).

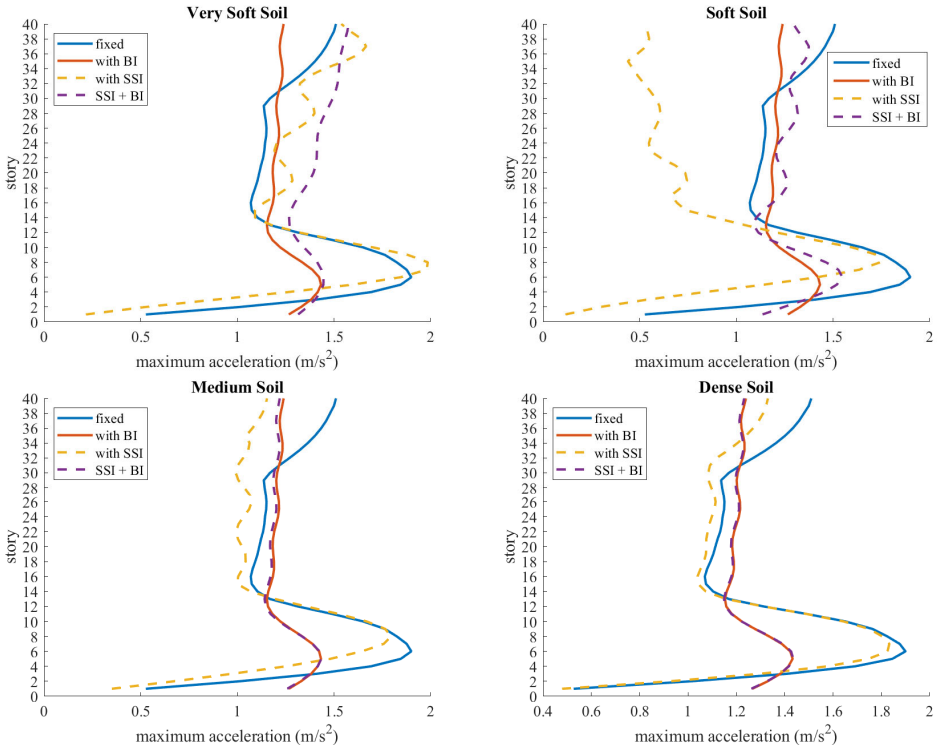

Figure 9. Maximum acceleration of each story for the forty-story building (Imperial Valley, 1979).

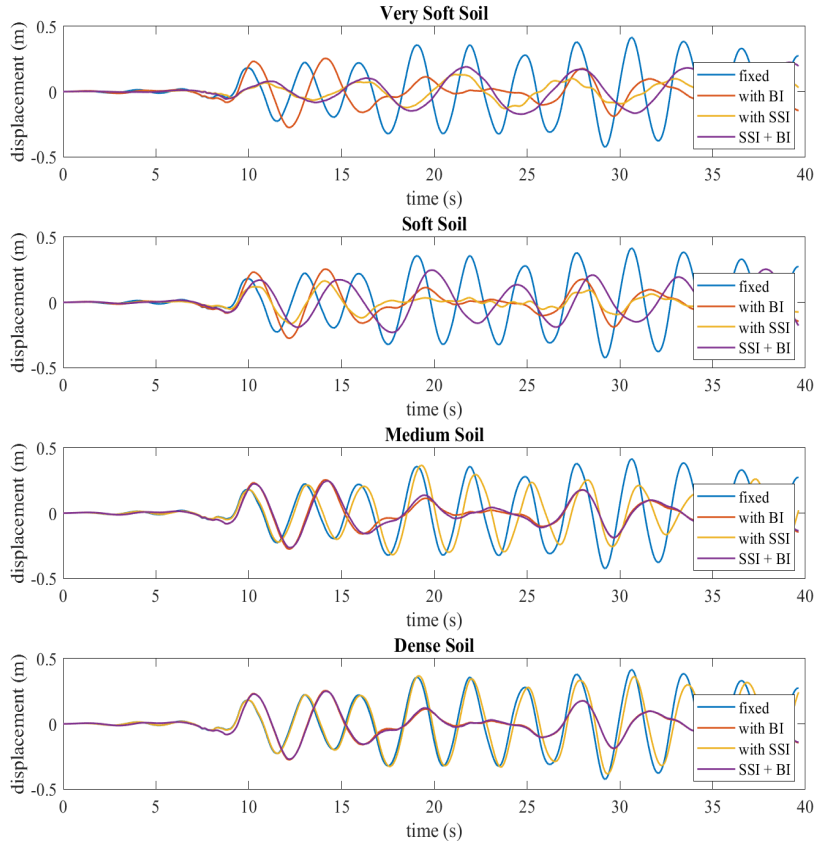

Figure 10. Top story displacement–time history of forty-story buildings (Imperial Valley, 1979).

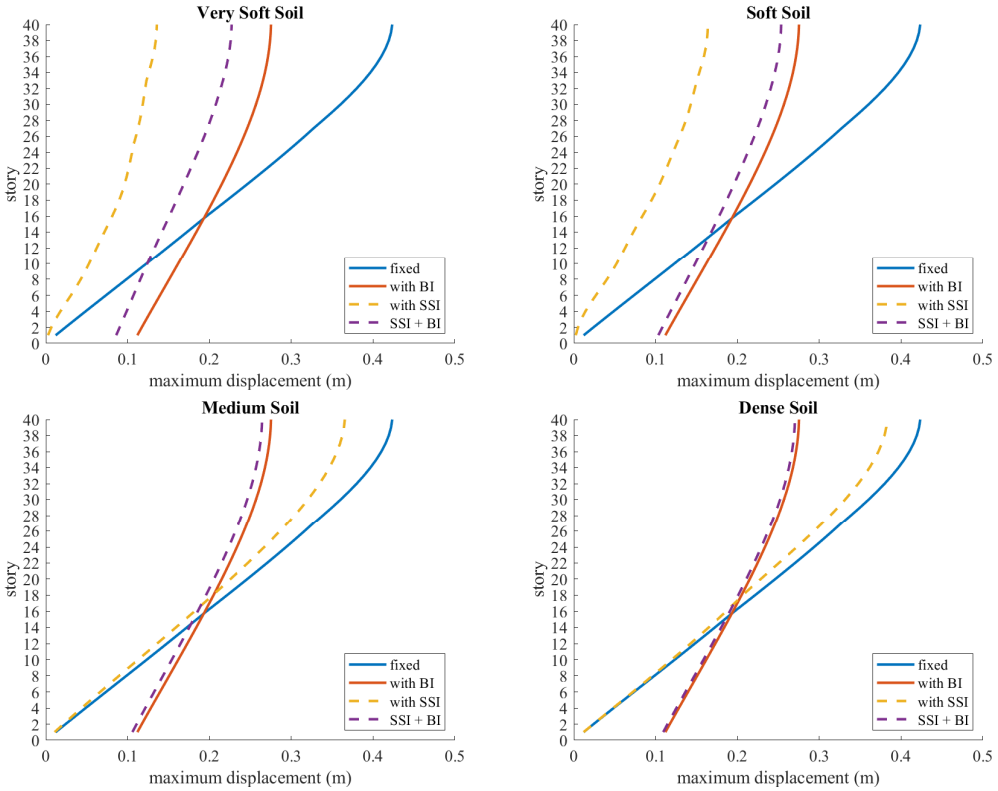

Figure 11. Maximum displacement of each story for the forty-story building (Imperial Valley, 1979).

Spectral Analysis

Spectral analyses are conducted for the five-story building considering the 1940 Imperial Valley earthquake. Spectral acceleration and displacement graphics can be seen in Figure 12. The results show that the period elongation feature of BI and SSI lowers the spectral acceleration response of the structure. BI displacements are higher than fixed conditions, which is the same as the time history results. We can also see that SSI effects are more noticeable in softer soil conditions, in a similar manner to time history results and that the effects diminish when we move towards denser soil. Table 9 shows the detailed results of the spectral analyses. In Table 9, T is the period, and SA, SV and SD are the spectral acceleration, spectral velocity and spectral displacement, respectively. If we consider Table 9 and Figure 12 for very soft soil conditions, the values of SA range from 1.84 to 5.34 with respect to the base conditions; for soft soil conditions, values of SA range from 1.92 to 5.34 with respect to the base conditions, for medium soil values of SA range from 1.92 to 5.45, which are the maximum obtained SA values among all the different soil conditions. Lastly, for dense soil, SA values range from 1.92 to 5.39. It can be observed from the table that when the period of the structure increases, SA decreases. This is applicable to all different soil conditions. BI cases have higher SA in all soil conditions. However, for spectral displacements, we can observe that when the period increases, the spectral displacement also increases. BI implementation increases SD, and this is the expected result. For all different soil types, this increase can be observed. The conclusions obtained from this study are presented in the next section.

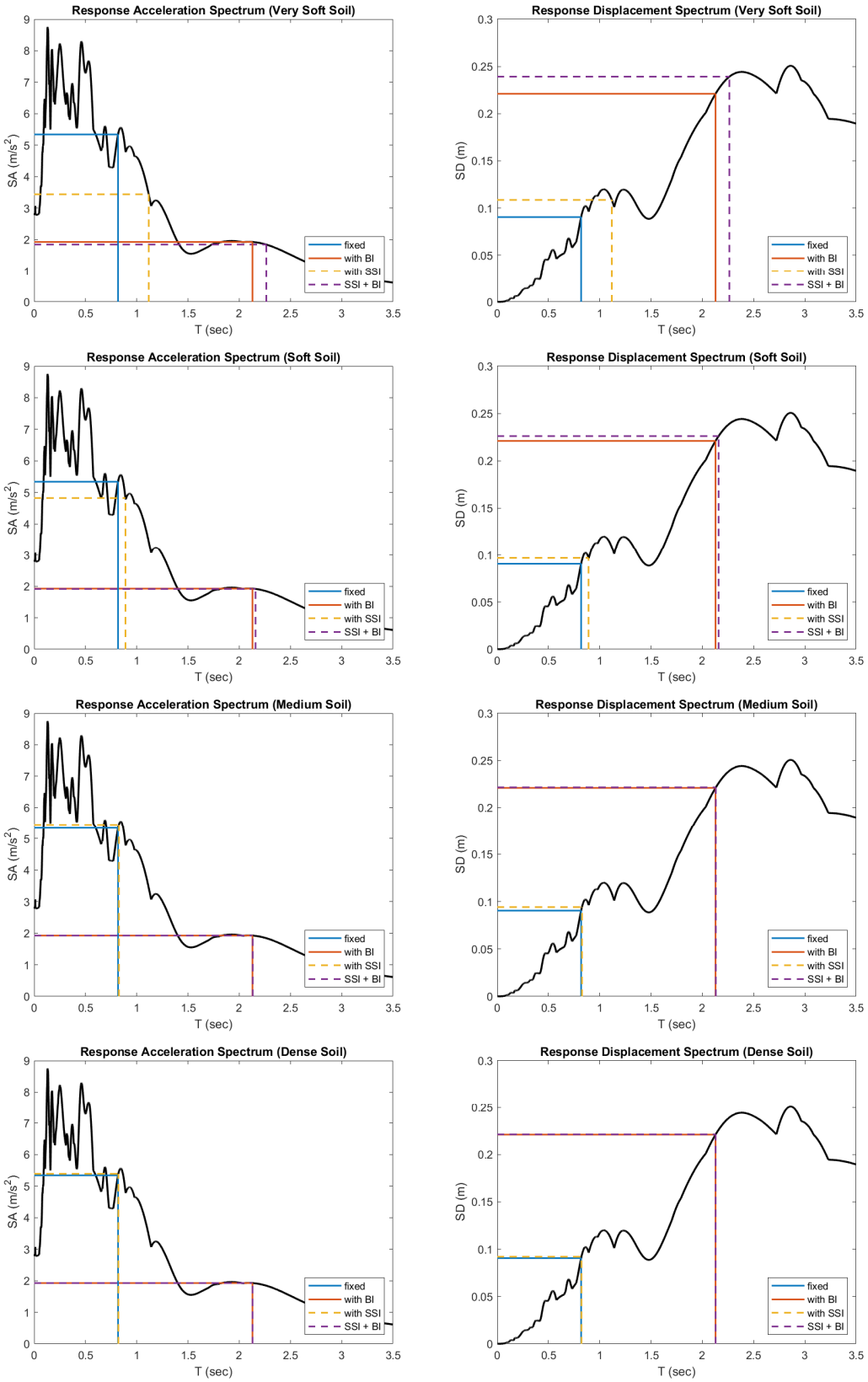

Figure 12. Spectral acceleration and displacement graphics for every soil condition.

Table 9. Spectral analysis results of the five-story building (Imperial Valley, 1940).

Soil	Base	T (s)	SA (m/s^2)	SV (m/s)	SD (m)
Very Soft Soil	fixed	0.82	5.34	0.70	0.09
Very Soft Soil	BI	2.13	1.93	0.65	0.22
Very Soft Soil	SSI	1.12	3.44	0.61	0.11
Very Soft Soil	SSI+BI	2.26	1.84	0.66	0.24
Soft Soil	fixed	0.82	5.34	0.70	0.09
Soft Soil	BI	2.13	1.93	0.65	0.22
Soft Soil	SSI	0.89	4.82	0.68	0.10
Soft Soil	SSI+BI	2.16	1.92	0.66	0.23
Medium Soil	fixed	0.82	5.34	0.70	0.09
Medium Soil	BI	2.13	1.93	0.65	0.22
Medium Soil	SSI	0.83	5.45	0.72	0.09
Medium Soil	SSI+BI	2.13	1.92	0.65	0.22
Dense Soil	fixed	0.82	5.34	0.70	0.09
Dense Soil	BI	2.13	1.93	0.65	0.22
Dense Soil	SSI	0.82	5.39	0.70	0.09
Dense Soil	SSI+BI	2.13	1.92	0.65	0.22

5. Conclusions

A large number of numerical analyses are conducted for three different buildings. With respect to the numerical results that are given in this paper, the following conclusions are obtained:

- BI may greatly reduce the acceleration, velocity and displacements of structures that are induced by earthquakes.
- Although the total displacement might be higher than in a fixed structure, most of it occurs on the isolation system, and the superstructure moves as a whole, resulting in much lower inter-story drift compared to the fixed base structure.
- SSI may modify the acceleration, velocity and displacement responses of structures.
- The results show that SSI mostly reduces the effects of earthquakes. In order to stay on the safer side, design codes do not specify SSI analysis procedures; they often briefly state that SSI can sometimes modify earthquake responses, and for those rare cases, it should be investigated.

This study's results are in line with these assumptions. For a small number of cases, SSI may slightly increase the response of structures. The results also show that SSI effects are much more pronounced in soft soil conditions and hardly ever present in dense soil conditions. In dense soil conditions, the response of structures eminently approaches that of fixed base conditions. Based on this study, SSI affects the performance of BI systems. The effectiveness of a BI system is reduced when SSI is considered. According to this study, both far and near-fault earthquakes lead to responses that have similar characteristics. The heights of the structures also do not have any significant effects when SSI and BI are considered together. Spectral analysis results are in line with the time history results.

The results obtained from this study are also compared with the existing literature. In this research, it is seen that SSI affects the performance of the isolation system. The same outcome was also obtained in [27,28,35]. Additionally, SSI effects were found to be more pronounced in soft soil conditions, which is similar to the findings presented in [13,14]. Moreover, our study includes many results about SSI effects on tall buildings. This is an important aspect of SSI research, as it was stated in [36] that SSI effects in tall buildings is a concept that needs to be investigated more.

Lastly, it should be mentioned that, by performing an extensive number of dynamic simulations that were coded based on the simple proposed formulation defined in Section 2.5, it was seen that the solution is computationally efficient, and it does not create any stability problems for the numerical model. For future studies, three-dimensional models considering SSI and BI can be studied. The formulation given in this study may also be generalized for three-dimensional structures considering SSI as a future study.

Author Contributions: Conceptualization, A.Y.; methodology, A.Y.; software, Y.U.; validation, Y.U. and A.Y.; formal analysis, Y.U.; investigation, A.Y. and Y.U.; resources, Y.U.; data curation, Y.U.; writing—original draft preparation, A.Y. and Y.U.; writing—review and editing, A.Y.; visualization, A.Y. and Y.U.; supervision, A.Y. All authors have read and agreed to the published version of the manuscript.

Funding: This research received no external funding.

Data Availability Statement: The data presented in this study are available on request from the corresponding author.

Conflicts of Interest: The authors declare no conflict of interest.

References

1. Chopra, A.K. *Dynamics of Structures, Theory and Applications to Earthquake Engineering*, 4th ed.; Pearson Education Limited: Upper Saddle River, NJ, USA, 2013.
2. American Society of Civil Engineers (ASCE). *Fema 356 Prestandard and Commentary for the Seismic Rehabilitation of Buildings*; Federal Emergency Management Agency: Washington, DC, USA, 2000.
3. Constantinou, M.C.; Kneifati, M.C. Dynamics of Soil-Base-Isolated-Structure Systems. *J. Struct. Eng.* **1988**, *114*, 211–221. [CrossRef]
4. Bycroft, G.N. Soil-structure interaction at higher frequency factors. *Earthq. Eng. Struct. Dyn.* **1977**, *5*, 235–248. [CrossRef]
5. Novak, M.; Henderson, P. Base-isolated buildings with soil-structure interaction. *Earthq. Eng. Struct. Dyn.* **1989**, *18*, 751–765. [CrossRef]
6. Pappin, J.W.; Lubkowski, Z.A.; King, R.A. The Significance of Site Response Effects on Performance Based Design. In Proceedings of the 12th World Conference on Earthquake Engineering, Auckland, New Zealand, 30 January–4 February 2000.
7. Mylonakis, G.; Gazetas, G. Seismic Soil-Structure Interaction: Beneficial or Detrimental? *J. Earthq. Eng.* **2000**, *4*, 277–301. [CrossRef]
8. Tongaonkar, N.; Jangid, R. Seismic response of isolated bridges with soil–structure interaction. *Soil Dyn. Earthq. Eng.* **2003**, *23*, 287–302. [CrossRef]
9. Mylonakis, G.; Voyagaki, E.; Price, T. Damage Potential of the 1999 Athens, Greece, Accelerograms. *Bull. Earthq. Eng.* **2003**, *1*, 205–240. [CrossRef]
10. Syngros, K. Seismic Response of Piles and Pile-Supported Bridge Piers Evaluated through Case Histories. Ph.D. Thesis, The City University of New York, New York, NY, USA, 2004.
11. Deb, S. Seismic base isolation—An overview. *Curr. Sci.* **2004**, *87*, 1426–1430. Available online: http://www.jstor.org/stable/24109483 (accessed on 5 July 2019).
12. Tsai, C.S.; Chen, C.-S.; Chen, B.-J. Effects of unbounded media on seismic responses of FPS-isolated structures. *Struct. Control Health Monit.* **2004**, *11*, 1–20. [CrossRef]
13. Dicleli, M.; Albhaisi, S.; Mansour, M.Y. Static Soil–Structure Interaction Effects in Seismic-Isolated Bridges. *Pract. Period. Struct. Des. Constr.* **2005**, *10*, 22–33. [CrossRef]
14. Liu, M.-Y.; Chiang, W.-L.; Hwang, J.-H.; Chu, C.-R. Wind-induced vibration of high-rise building with tuned mass damper including soil–structure interaction. *J. Wind. Eng. Ind. Aerodyn.* **2008**, *96*, 1092–1102. [CrossRef]
15. Spyrakos, C.; Koutromanos, I.; Maniatakis, C. Seismic response of base-isolated buildings including soil–structure interaction. *Soil Dyn. Earthq. Eng.* **2009**, *29*, 658–668. [CrossRef]
16. Jeremić, B.; Jie, G.; Preisig, M.; Tafazzoli, N. Time domain simulation of soil-foundation-structure interaction in non-uniform soils. *Earthq. Eng. Struct. Dyn.* **2009**, *38*, 699–718. [CrossRef]
17. Karabörk, T.; Deneme, İ.Ö.; Bilgehan, R.P. Dynamic soil structure interaction analysis for base isolated structures. *Erciyes Univ. J. Inst. Sci. Technol.* **2010**, *26*, 77–87.
18. Kausel, E. Early history of soil–structure interaction. *Soil Dyn. Earthq. Eng.* **2010**, *30*, 822–832. [CrossRef]
19. Genes, M.; Doğanay, E.; Bikçe, M.; Kaçın, S. Soil-Structure Interaction in RC Frame Buildings from Strong-Motion Recordings. *KSU J. Eng. Sci.* **2011**, *14*, 1–7. Available online: http://jes.ksu.edu.tr/en/download/article-file/180955 (accessed on 9 August 2019).
20. Matinmanesh, H.; Asheghabadi, M.S. Seismic Analysis on Soil-Structure Interaction of Buildings over Sandy Soil. *Procedia Eng.* **2011**, *14*, 1737–1743. [CrossRef]
21. Manolis, G.D.; Markou, A. A distributed mass structural system for soil-structure-interaction and base isolation studies. *Arch. Appl. Mech.* **2012**, *82*, 1513–1529. [CrossRef]
22. Giarlelis, C.; Mylonakis, G. The role of soil-structure interaction in the inelastic performance of multi-story buildings. In Proceedings of the 9th International Conference on Structural Dynamics, EURODYN 2014, Porto, Portugal, 30 June–2 July 2014.
23. Li, C.P.; Liu, W.Q.; Wang, S.G.; Du, D.S. Analysis of Soil-Structure Interaction (SSI) Effects on Seismic Response of Base-Isolated Structures. *Adv. Mater. Res.* **2010**, *163–167*, 4199–4207. [CrossRef]
24. Luco, J.E. Effects of soil–structure interaction on seismic base isolation. *Soil Dyn. Earthq. Eng.* **2014**, *66*, 167–177. [CrossRef]
25. Tsai, C.S.; Hsueh, C.I.; Su, H.C. Roles of soil-structure interaction and damping in base-isolated structures built on numerous soil layers overlying a half-space. *Earthq. Eng. Eng. Vib.* **2016**, *15*, 387–400. [CrossRef]

26. Yanik, A. Absolute Instantaneous Optimal Control Performance Index for Active Vibration Control of Structures under Seismic Excitation. *Shock Vib.* **2019**, *2019*, 4207427. [CrossRef]
27. Ashiquzzaman; Hong, K.-J. Simplified Model of Soil-Structure Interaction for Seismically Isolated Containment Buildings in Nuclear Power Plant. *Structures* **2017**, *10*, 209–218. [CrossRef]
28. Zhou, Z.; Wei, X. Seismic Soil-Structure Interaction Analysis of Isolated Nuclear Power Plants in Frequency Domain. *Shock Vib.* **2016**, *2016*, 6127895. [CrossRef]
29. Zhao, X.; Wang, S.; Du, D.; Liu, W. Optimal Design of Viscoelastic Dampers in Frame Structures considering Soil-Structure Interaction Effect. *Shock Vib.* **2017**, *2017*, 9629083. [CrossRef]
30. Forcellini, D. Seismic assessment of a benchmark based isolated ordinary building with soil structure interaction. *Bull. Earthq. Eng.* **2018**, *16*, 2021–2042. [CrossRef]
31. McKenna, F. OpenSees: A Framework for Earthquake Engineering Simulation. *Comput. Sci. Eng.* **2011**, *13*, 58–66. [CrossRef]
32. Dai, W.; Rojas, F.; Shi, C.; Tan, Y. Effect of soil structure interaction on the dynamic responses of base isolated bridges and comparison to experimental results. *Soil Dyn. Earthq. Eng.* **2018**, *114*, 242–252. [CrossRef]
33. El-Sinawi, A.H.; AlHamaydeh, M.H.; Jhemi, A.A. Optimal Control of Magnetorheological Fluid Dampers for Seismic Isolation of Structures. *Math. Probl. Eng.* **2013**, *2013*, 251935. [CrossRef]
34. Yanik, A. Seismic control performance indices for magneto-rheological dampers considering simple soil-structure interaction. *Soil Dyn. Earthq. Eng.* **2020**, *129*, 105964. [CrossRef]
35. Zhenxia, S.; Haiping, D. The Analysis of Seismic Response for Base-isolated Structure by LS-DYNA. Indian Institute of Technology Kanpur. Available online: http://www.iitk.ac.in/nicee/wcee/artical/14_14-0204.pdf (accessed on 7 August 2019).
36. Forcellini, D. Seismic fragility of tall buildings considering soil structure interaction (SSI) effects. *Structures* **2022**, *45*, 999–1011. [CrossRef]
37. Jalali, H.H.; Farzam, M.F.; Gavgani, S.A.M.; Bekdaş, G. Semi-active control of buildings using different control algorithms considering SSI. *J. Build. Eng.* **2023**, *67*, 105956. [CrossRef]
38. Maleska, T.; Beben, D. Behaviour of Soil–Steel Composite Bridges under Strong Seismic Excitation with Various Boundary Conditions. *Materials* **2023**, *16*, 650. [CrossRef]
39. Wang, J.; Xie, Y.; Guo, T.; Du, Z. Predicting the Influence of Soil–Structure Interaction on Seismic Responses of Reinforced Concrete Frame Buildings Using Convolutional Neural Network. *Buildings* **2023**, *13*, 564. [CrossRef]
40. Jin, L.; Li, B.; Lin, S.; Li, G. Optimal Design Formula for Tuned Mass Damper Based on an Analytical Solution of Interaction between Soil and Structure with Rigid Foundation Subjected to Plane SH-Waves. *Buildings* **2022**, *13*, 17. [CrossRef]
41. Deng, Y.; Ge, S.; Lei, F. Effects of Pounding and Abutment Behavior on Seismic Response of Multi-Span Bridge Considering Abutment-Soil-Foundation-Structure Interactions. *Buildings* **2023**, *13*, 260. [CrossRef]
42. Datta, T.K. *Seismic Analysis of Structures*; John Wiley & Sons (Asia) Pte Ltd.: Singapore, 2010.
43. Pioldi, F.; Salvi, J.; Rizzi, E. Refined FDD modal dynamic identification from earthquake responses with Soil-Structure Interaction. *Int. J. Mech. Sci.* **2017**, *127*, 47–61. [CrossRef]
44. Bekdaş, G.; Nigdeli, S.M. Metaheuristic based optimization of tuned mass dampers under earthquake excitation by considering soil-structure interaction. *Soil Dyn. Earthq. Eng.* **2017**, *92*, 443–461. [CrossRef]
45. Salvi, J.; Pioldi, F.; Rizzi, E. Optimum Tuned Mass Dampers under seismic Soil-Structure Interaction. *Soil Dyn. Earthq. Eng.* **2018**, *114*, 576–597. [CrossRef]
46. Pacific Earthquake Engineering Research Center. PEER NGA-West2 Database. Available online: https://ngawest2.berkeley.edu/ (accessed on 2 July 2019).
47. Cardone, D.; Viggiani, L.; Perrone, G.; Telesca, A.; Di Cesare, A.; Ponzo, F.; Ragni, L.; Micozzi, F.; Dall'Asta, A.; Furinghetti, M.; et al. Modelling and Seismic Response Analysis of Existing Italian Residential RC Buildings Retrofitted by Seismic Isolation. *J. Earthq. Eng.* **2023**, *27*, 1069–1093. [CrossRef]
48. Cardone, D.; Conte, N.; Dall'Asta, A.; Di Cesare, A.; Flora, A.; Lamarucciola, N.; Micozzi, F.; Ponzo, F.C.; Ragni, L. RINTC-E project: The seismic risk of existing Italian RC buildings retrofitted with seismic isolation. In Proceedings of the 7th ECCOMAS Thematic Conference on Computational Methods in Structural Dynamics and Earthquake Engineering, COMPDYN 2019, Crete, Greece, 24–26 June 2019.
49. Iervolino, I.; Spillatura, A.; Bazzurro, P. Seismic Reliability of Code-Conforming Italian Buildings. *J. Earthq. Eng.* **2018**, *22*, 5–27. [CrossRef]
50. Calvi, P.M.; Calvi, G.M. Historical development of friction-based seismic isolation systems. *Soil Dyn. Earthq. Eng.* **2018**, *106*, 14–30. [CrossRef]